JOURNAL OF MATERIALS SCIENCE 23 (1988) 4076–4080

Crystallization kinetics of amorphous $Ni_{78}P_{22}$ powders and hydrogen adsorption on both amorphous and crystal alloy powders

M. V. ŠUŠIĆ
Institute of Physical Chemistry, Faculty of Sciences, Studentski trg 16, 11000 Belgrade, Yugoslavia

D. P. USKOKOVIĆ
Institute of Technical Sciences of the Serbian Academy of Sciences and Arts, Knez Mihailova 35, 11000 Belgrade, Yugoslavia

A thermal and kinetic investigation of the behaviour of amorphous and crystal powder alloy $Ni_{78}P_{22}$ was performed in a hydrogen atomsphere. It was shown that the amorphous alloy absorbs hydrogen within the temperature range 393 to 520 K. After that it is transformed into the crystal (stable) state in two steps at 615 and 670 K, respectively, thus forming stable Ni and Ni_3P phases. The crystal form of the same sample also adsorbs hydrogen, but at lower temperatures ranging from 310 to 520 K. The activation energies of the crystallization process, as well as the frequency factors, the rate constants and the enthalpy of crystallization were determined. Both kinetic and thermal parameters of the hydrogen adsorption process taking place in at least two steps, as in the crystallization process, were also determined.

1. Introduction

Investigation of the thermal stability of amorphous powders has proved to be of particular importance because their use is mostly limited and requires various methods of consolidation that can cause their transformation into the crystal state [1], whether consolidation is performed under "cold" or "warm" conditions. This has been particularly requested when production of theoretically dense amorphous materials during consolidation processes is in question, when a change of state is forbidden [2]. Because of the reasons given above, investigation of the crystallization kinetics and stability offers a series of important data that are of great significance for the development and application of these materials.

The amorphous alloy $Ni_{100-x}P_x$ belongs to the group of amorphous alloys of transition metals with metalloids, and numerous data on it are available in literature. A sigmoidal behaviour of relative temperature coefficient of resistance dependent upon the phosphorus content [3] was shown using this alloy as an example. The alloy has been greatly investigated using the theory of vitreous state of sphere packing by a computer modelling method [4]. The eutectic mixture contains 18 at.% phosphorus; an alloy with a lower or greater phosphorus content exhibits different magnetic properties, i.e. the alloy containing < 18 at.% phosphorus possesses the properties that are characteristic of amorphous ferromagnets (indicative of homogeneous systems). The clustered nickel appears in an otherwise paramagnetic matrix [5] in alloys with > 18 at.% phosphorus. The importance of studying the "amorphous, microcrystalline and vitreous" state, dealing with the structure of amorphous and microcrystalline material such as Pt–C and "amorphous" Ni–P powder obtained by electroless deposition, similar to our sample, should be stressed [6]. It is evident [7, 8] that for $Ni_{80}P_{20}$, vitreous transition occurs at $T_g = 618$ K (extrapolated), the eutectic at 770 K, but not at the crystallization temperature.

In this paper we report the investigation of the crystallization kinetics of amorphous $Ni_{78}P_{22}$ powder alloy as well as the hydrogen adsorption kinetics of both amorphous and crystallized forms.

2. Experimental procedure

The amorphous Ni–P powder obtained by electroless reduction of di-valent nickel ions by sodium hypophosphite in buffered aqueous solution at 380 K was studied. The composition of the alloy depends on reduction conditions and particularly on the content of phosphorus and the pH of the solution. The product obtained contained 14 wt% phosphorus which corresponds, according to the Ni–P phase diagram [9], to the composition of $Ni_{78}P_{22}$. Because of the content of phosphorus, this somewhat exceeds the composition of eutectic Ni–P (18 at.%). The crystallization kinetics was analysed by differential scanning calorimetry (DSC) using a Dupont Thermal Analyser 1090 in a hydrogen atmosphere. The change in structure occurring during crystallization and hydrogen adsorption was investigated by X-ray diffraction using Cu$K\alpha$ radiation and a graphite monochromator.

3. Results and discussion

When heating samples of 15 to 30 mg in a DSC cell in

0022–2461/88 $03.00 + .12

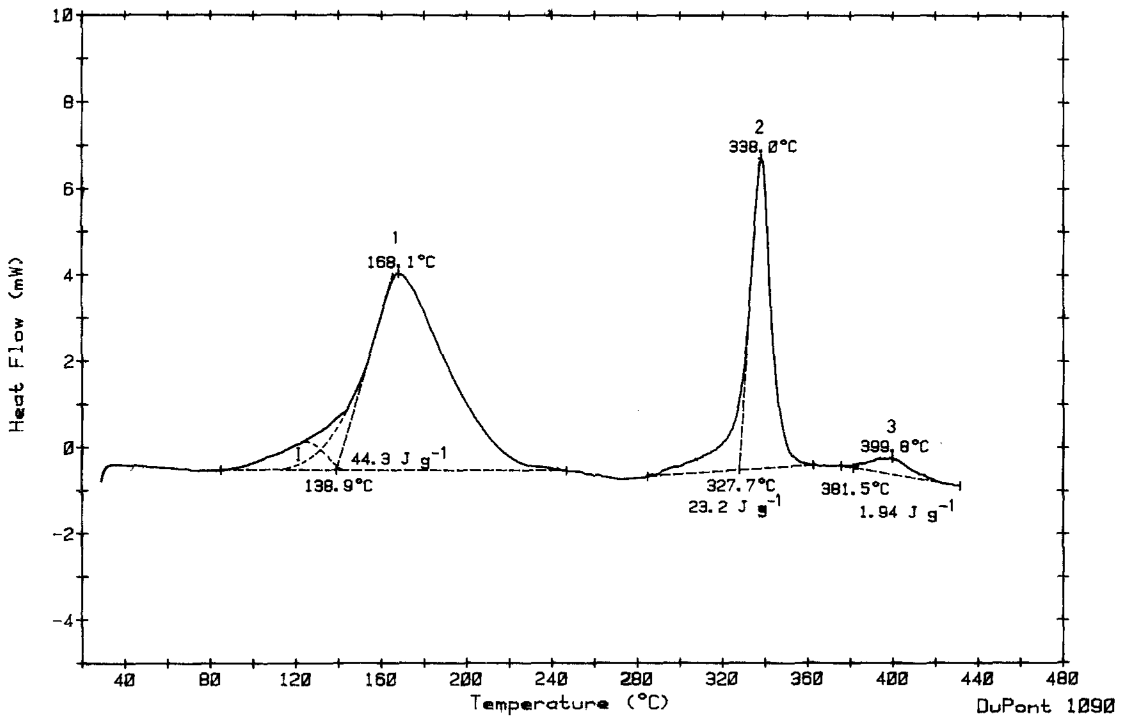

Figure 1 DSC thermogram of amorphous powder $Ni_{78}P_{22}$ in H_2, 15 K min^{-1}.

a hydrogen atmosphere, a thermogram with three exothermal maxima, denoted by 1, 2 and 3, at the corresponding different temperatures (Fig. 1) were obtained. After reheating the cooled sample which was exposed to the air for 10 to 15 min, we obtained a thermogram with only one exothermal maximum 1, Fig. 2. As is evident from Fig. 3, X-ray analysis shows that the investigated powder is amorphous and that it transformed into the crystal state during heating. The first maximum on the thermogram corresponds to hydrogen adsorption on the amorphous sample (Fig. 1) and to that on the crystallized sample (Fig. 2). The second maximum and the third small maximum correspond to the crystallization process and recrystallization (complete stabilization) of the polycrystalline products Ni and Ni_3P formed as shown in Fig. 3 and as reported by Diximer and Guinier [6], according to whom nickel and then Ni_3P crystals are formed because of the amorphous mass. Thus the third maximum is attributed to the process of further stabilization of the crystal state. The vitreous transition, T_g, occurs at 578 K when $\beta = 40$ K min^{-1} and is visible only at higher heating rates.

The crystallization kinetics was analysed by the method given by Barker [10], according to which the relation $\log(\beta/T^2) - 1/T$ is linear where β is the heating rate of the sample and T is the peak temperature of the exothermal maximum. The activation energy of the

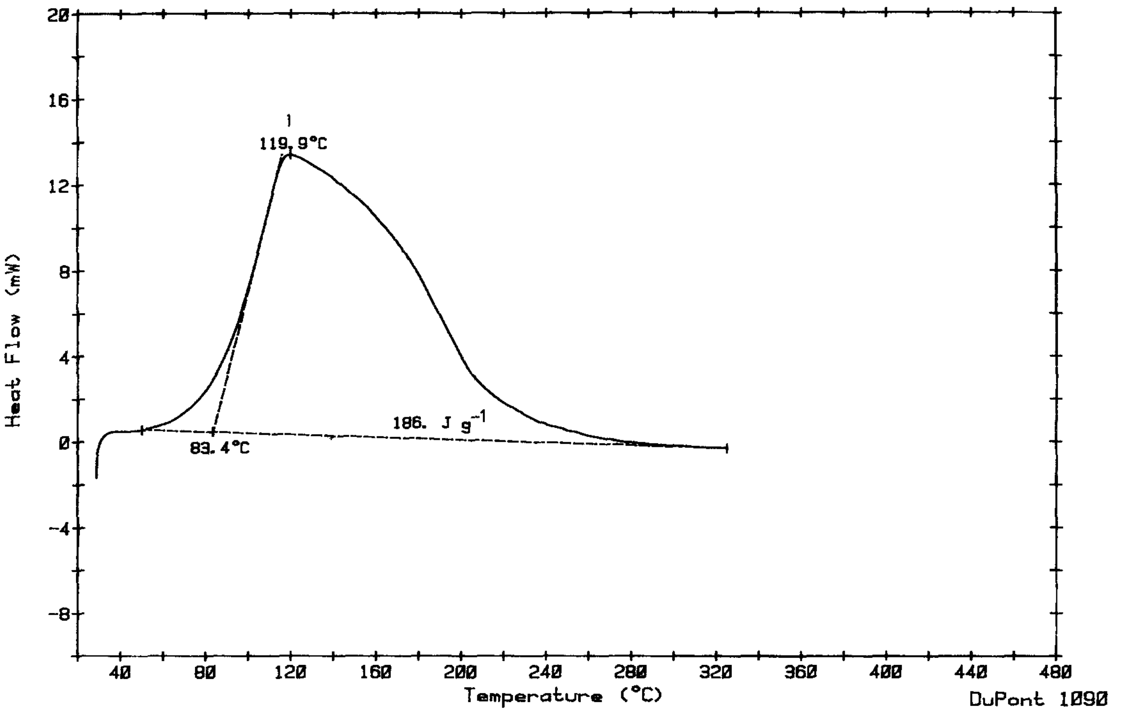

Figure 2 DSC thermogram of the same powder $Ni_{78}P_{22}$ after crystallization in H_2, 15 K min^{-1}. (Fig. 1)

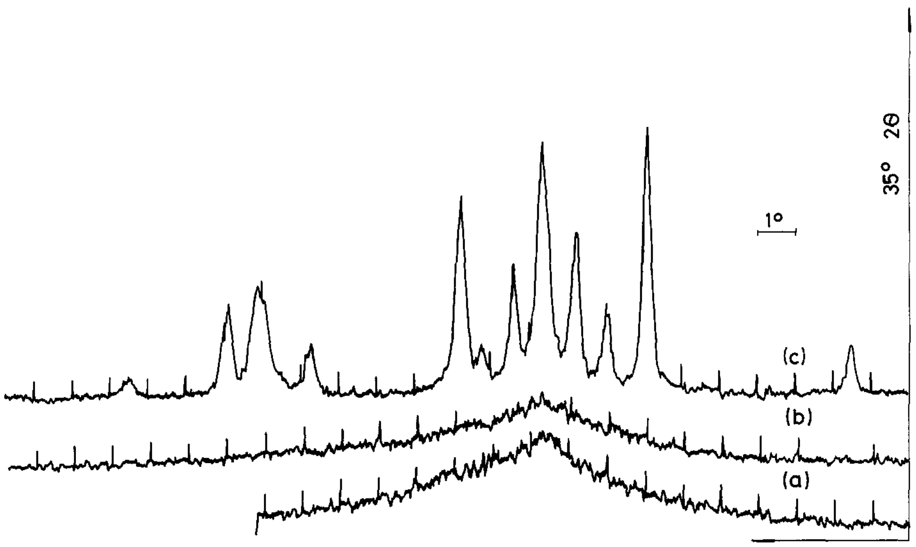

Figure 3 X-ray diffractograms of Ni_{78}–P_{22} powder: (a) before heating, (b) after hydrogen adsorption and (c) after crystallization.

crystallization process, E, can be derived from the slope. The frequency factor, Z, is calculated from the relation $Z = [\beta E \exp(E/RT)]/RT^2$ and the crystallization rate constant, k, is determined from the relation $k = Z \exp(-E/RT)$. It was shown that this means of analysis can be applied, as a plot of $\log(\beta/T^2)$ against $1/T$ yields a straight line (Fig. 4). Slopes of $\Delta \log(\beta/T^2)/\Delta(1/T)$ equal to -11.09×10^3 for the second and -10.77×10^3 for the third maximum are derived from this plot and on the basis of these the corresponding activation energies $E_2 = 212.36$ and $E_3 = 206.26\,\mathrm{kJ\,mol^{-1}}$ are found as well as (for $\beta = 20\,\mathrm{K\,min^{-1}}$) the frequent factors $Z_2 = 9.66 \times 10^{17}\,\mathrm{min^{-1}}$ at 621 K and $Z_3 = 5.99 \times 10^{15}\,\mathrm{min^{-1}}$ at 684 K. The corresponding rate constants at a maximum peak were found to be $k_2 = 1.324$ and $k_3 = 1.060\,\mathrm{min^{-1}}$. The change in rate constants is followed by a change in temperature as seen from Fig. 4b. It is obvious from the results that the activation energies are rather high, as are the frequency factors. The high rate constants of the crystallization process should certainly be underlined. The enthalpies are found to be $\Delta H_2 = -23\,\mathrm{J\,g^{-1}}$ for the first and $\Delta H_3 = 2.5\,\mathrm{J\,g^{-1}}$ for the second crystallization step. The great difference that exists between enthalpy values proves that the third maximum (second crystallization step) can be attributed to the recrystallization–stabilization process of the polycrystallites formed in the first step. This method proved to be not sufficiently reliable for investigation of the hydrogen absorption kinetics process.

Further investigations have stated that both amorphous and crystalline forms are active hydrogen adsorbers and the first maximum, given in Fig. 1, is ascribed to that fact. Investigation of hydrogen adsorption kinetics was previously performed on the basis of non-isothermal differential thermal analysis (DTA), but in this paper the DSC method was used. Thus according to Borchardt and Farrington [11] for certain chemical reactions of the first order, the rate constant $k = (\Delta H/\Delta t)/(A - a)$ plotted against $1/T$ yields a straight line, the slope of which gives the activation energy and other kinetic values can be obtained, where ΔH is the enthalpy, t the time, A the total area below the maximum in the thermogram, and a is the area below the maximum registered by a recorder in time t of the reaction). $\Delta H/\Delta t$ is the slope of a tangent at the maximum in time t. The DSC method we used gives the relationship $k = \Delta mW(A - a)$ for the rate constant where ΔmW is the value of the ordinate for the corresponding temperature (time) in milliwats. This is

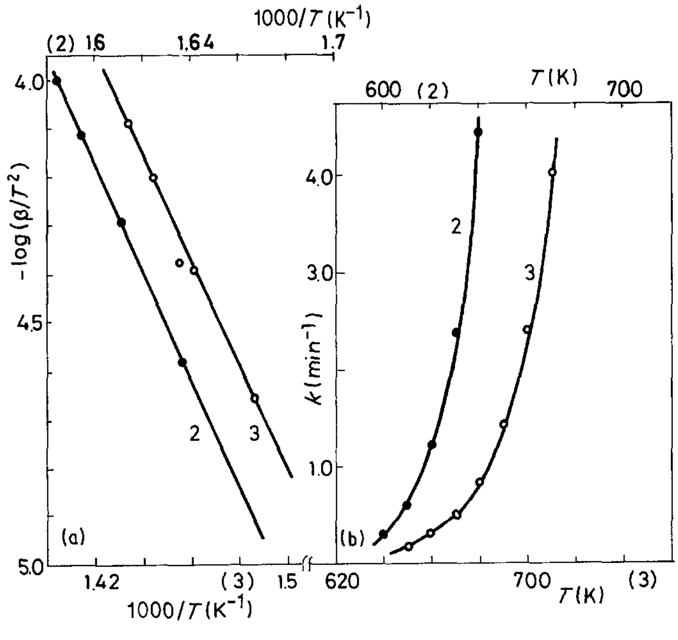

Figure 4 (a) Energy activation plot $\log(\beta/T^2)$ against $1/T$, and (b) dependence of a rate constant on temperature for the crystallization process.

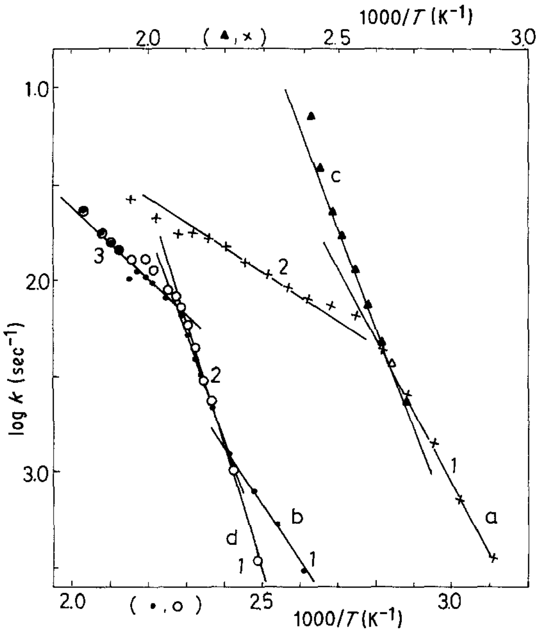

Figure 5 Energy activation plot log k against $1/T$ for hydrogen adsorption on amorphous and crystallized, in hydrogen, powder $Ni_{78}P_{22}$. Amorphous Ni–P: see Fig. 1, (●) analysis of total exothermal-maximum (straight line b), (○) omitted first part of maximum I (straight line d), (▲) the first part of I only (straight line c): Crystalline $Ni_{78}P_{22}$: (x) analysis of maximum in Fig. 2 (straight line a).

applicable only if the hydrogen adsorption process is of the first order (along with the corresponding negligence of some less important parameters).

When observing the exothermal maximum 1 in Fig. 1 a considerable asymmetry is noticed at the beginning of the adsorption process which originates from the exothermal process (denoted I) being of lower intensity than the total exothermal maximum. We suppose that this effect (which is not evident in the same sample crystallized in hydrogen) results from the activation process of the amorphous sample for hydrogen adsorption. Analysis of the total exothermal-maximum carried out as above, gives the straight line b, in Fig. 5, having three slopes 1, 2 and 3 which should indicate three steps of the process. The corresponding activation energies, $E_1 = 56.73$, $E_2 = 108.50$ and $E_3 = 34.19\,\mathrm{kJ\,mol^{-1}}$, were determined from this slope. However, analysis of the very graphically separated part I, Fig. 1, gives an activation energy $E = 99.98\,\mathrm{kJ\,mol^{-1}}$ from the slope of line c (Fig. 5). When surface I is subtracted from the total surface of exo-maximum and the rest is analysed, we obtain the straight line d, (Fig.5), from the slope (1) of which we found the activation energy $E_1 = 118.84\,\mathrm{kJ\,mol^{-1}}$. This is very similar to the activation energy E_2 resulting from the straight line b. The second slope, 2, of the straight line d practically overlaps the slope of the straight line b. It can be stated on the basis of these results that the real hydrogen adsorption process on amorphous Ni–P powder occurs as a first-order reaction.

Hydrogen adsorption on a crystallized sample, after crystallization of amorphous powder in hydrogen, takes place in two steps (Fig. 2) with different activation energies. As is evident from Fig. 5, the activation energy $E_1 = 68.95\,\mathrm{kJ\,mol^{-1}}$ for the first step (lower temperature) and that for the second step $E_2 = 25.53\,\mathrm{kJ\,mol^{-1}}$ is calculated from slopes 1 and 2 of the straight line a. It is obvious even from visual observation of the analysed thermogram in Fig. 2, that the process takes place in two steps at least. It can also be established that monohydrides are formed in the first step, while di- or poly-hydrides are formed in the second. The shape of the exothermal-maximum is very similar to the exothermal-maximum of hydrogen adsorption on NiZr and CoZr alloys [12]. Therefore, on the basis of data obtained it can be concluded that the hydrogen adsorption mechanism on amorphous and crystalline Ni–P powder does not differ in essence, although some distinctions are seen: when amorphous powder is concerned, the activation process that precedes the first, predominant step, exists, while the crystalline powder is deprived of the activation (but is activated during the crystallization process) and the second step is expressed well. The enthalpies of the hydrogen adsorption process are mutually different and are 170 to $190\,\mathrm{J\,g^{-1}}$ approximately for a crystalline system and $45\,\mathrm{J\,g^{-1}}$ approximately for an amorphous system. The lower enthalpy of the amorphous sample originates from the fact that the sample suffers no activation. The experimental results also show that there is no difference in the adsorption energy of the activated amorphous sample and that after crystallization. The results obtained indicate this material should be considered an important hydrogen adsorbent at temperatures ranging from 320 to 520 K.

4. Conclusion

The crystallization kinetics of the amorphous alloy $Ni_{78}P_{22}$ in a dispersed state and that of hydrogen adsorption in both the amorphous and crystalline states, were thoroughly investigated by differential scanning calorimetry and X-ray diffraction. It was shown that an amorphous alloy absorbs hydrogen within the temperature interval 393 to 520 K and is then transformed, through two steps, to the crystalline state at temperatures of 615 and 670 K. The crystal form of the same sample also absorbs hydrogen, in a somewhat lower temperature field from 310 to 520 K. The kinetic parameters of both crystallization and hydrogen adsorption processes which take place in at least two steps, were determined.

Acknowledgements

The investigations presented in this paper were financially supported by the Republic Committee for the Science of Serbia through the project "Physical Chemistry of Condensed Systems". The authors are grateful to Ms V. Pejović from the Institute of Electronic Industry for supplying Ni–P powders.

References

1. S. A. MILLER, Amorphous Structures and their Formation and Stability, in "Amorphous Metallic Alloys", edited by F. E. Luborsky (Butterworths, 1983) p. 506.
2. D. G. MORRIS, *Metal Sci. J.* **14** (1980) 215.
3. P. J. COTE, *Solid State Commun.* **18** (1976) 1311.
4. G. S. CARGILL, *J. Appl. Phys.* **41** (1970) 2248.
5. A. BERADA, M. E. LAPIERRE, B. LOEGEL, P. PANISSOD and C. ROBERT, *J. Appl. Phys. F* **8** (1978) 845.

6. J. DIXMIER and A. GUINIER, *Fizika* **2** Suppl. 2 (1970) 9.1.
7. H. S. CHEN, *Acta Metall.* **22** (1974) 897.
8. *Idem, ibid.* **22** (1974) 1505.
9. G. V. SAMSONOV and I. M. VINICKII, "Tugoplavkie Soedineniya" (Metallurgiya, Moscow, 1976) p. 521.
10. K. F. BARKER, "Thermal Stability of Potentially Hazardous Materials by Differential Scanning Calorimetry (DSC)", DuPont Com. Instr. Products, Scientific and Process Division, Wilmington, Number TA 73, DE 19898.
11. H. J. BORCHARDT and D. FARRINGTON, *J. Amer. Chem. Soc.* **79** (1957) 41.
12. M. V. ŠUŠIC, to be published.

*Received 24 September
and accepted 22 October 1987*